1086 | https://doi.org/10.3311/PPci.24741
Creative Commons Attribution

Periodica Polytechnica Civil Engineering, 68(4), pp. 1086–1097, 2024

Shear Lag Effect and Its Additional Deflection Contribution of Composite Beam Bridges

Pengzhen Lu[1], Zhenyi Qi[1], Ying Wu[2*], Yu Ding[1], Liu Yang[1], Yang Li[1]

[1] School of Civil Engineering, Zhejiang University of Technology, No. 288 Liuhe Road, Xihu District, Hangzhou 310023, Zhejiang Province, China
[2] College of Information Engineering, Jiaxing Nanhu University, No. 572 Yuexiu South Road, Nanhu District, Jiaxing 314001, Zhejiang Province, China
* Corresponding author, e-mail: wy43601@163.com

Received: 26 December 2023, Accepted: 25 March 2024, Published online: 11 June 2024

Abstract

The composite beam structure is widely used in the engineering field because it benefits from the advantages of two materials, presenting outstanding advantages for construction purposes. However, at present, there are issues with the analysis and solution of the composite beam structure, such as the difficulty in developing a suitable analytical theory and the low degree of refinement achieved by simulation analysis. To accurately grasp the mechanical behavior of the composite beam structure and achieve its refined analysis, this paper proposes a refined spatial grid element analysis method that can simultaneously obtain the internal forces, displacements, and stresses of various parts of a composite beam. Based on the above new method, the effects of geometrical structural factors such as wide-span ratio, high-span ratio, and web thickness with respect to the shear lag effect are analyzed. The distribution law of the shear lag coefficient and its additional deflection are analyzed. The results demonstrate that using this analysis method to calculate and analyze steel-concrete duplex type composite beams can directly obtain the internal forces and displacements of the joints of the composite beam roof, floor, and web. The spatial grid element analysis method provides both the theoretical and practical means to achieve both the overall and local refinement analysis of the composite beam structure.

Keywords

steel-concrete I-shaped composite beam, spatial grid element, MATLAB program design, refined analysis, shear lag effect

1 Introduction

With the comprehensive construction of China's infrastructure, steel-concrete composite beams are increasingly being used in civil buildings and bridge engineering owing to their advanced and reasonable structural form, lighter weight, large torsional stiffness, and good seismic and dynamic performance [1]. However, as the composite beam structure develops toward larger spans and wider flanges, some issues become more relevant, such as longitudinal cracking of concrete slabs, lateral cracking because of negative bending moments in continuous beams, partial rupture of concrete bridge decks, shearing of shearing keys, and deflection of main beams. In particular, the stress distribution of the cross-section of an I-beam composite beam bridge with large width does not satisfy the flat section assumption under an external load. Among these issues, the shear lag effect is a prominent problem. If the shear lag effect is not fully analyzed in the design process, it may seriously affect the structural performance and operational safety of composite beam structures.

Regarding these issues, some research has been carried out. Huang et al. [2] established a theoretical model of the long-term mechanical performance of prefabricated composite beams, and the age-adjusted effective modulus method is adopted according to the deformation coordination conditions of new and old concrete bridge deck beams and steel beams. Tian [3] discussed the calculation method of composite beam-bridge shear joints for various specifications. Su et al. [4] conducted a negative bending test on the steel-concrete composite deck test specimen, and studied the effects of steel fiber concrete (SFRC), reinforcement ratio, shear joint type and other factors. Elmy and Nakamura [5] conducted an experimental study on

Cite this article as: Lu, P., Qi, Z., Wu, Y., Ding, Y., Yang, L., Li, Y. "Shear Lag Effect and Its Additional Deflection Contribution of Composite Beam Bridges", Periodica Polytechnica Civil Engineering, 68(4), pp. 1086–1097, 2024. https://doi.org/10.3311/PPci.24741

some steel reinforced concrete bridge models, and established a finite element model that considers material nonlinearity and shear transfer between steel and concrete. Liu et al. [6] studied the influence of different lateral connection forms on the torsional performance of composite bridges, and the influence of different shapes of steel webs on the torsional performance of composite bridges. Kisała and Furtak [7] proposed a new program for evaluating the effect of slippage on the deflection of steel plate-concrete composite beams, and verified the correctness of the theoretical analysis through experimental studies. Zhang et al. [8] presents results from experimental and numerical studies on the response of steel-concrete composite box bridge girders under certain localized fire exposure conditions. Tong et al. [9] proposed a new calculation method for partial or total shear joint beam deflection. Zou et al. [10] derived the interface slip formula for a composite beam under uniform and concentrated loads by establishing a differential equation for interface slip and then running simulations using real boundary conditions. Liu et al. [11] and others studied the bending resistance of simply supported steel-concrete composite beams under a positive bending moment through a combination of tests and finite element modeling.

At present, the research on I-shaped composite beams has mainly focused on the overall mechanical performance, shear joints, concrete cracking, interface slip performance, etc. There is relatively little research on the shear lag effect on an I-shaped composite beam. Analytical methods and numerical methods are commonly used to analyze the shear lag effect of composite beams. Zhu and Su [12] proposed a new composite beam analysis method that can simulate the effects of interface slip and shear lag, as well as their time dependence; Luo et al. [13] investigated shear lag effect in steel-concrete composite beams sustaining hogging moment. A method was given specifically for predicting the effect in the cracked part of the steel-concrete composite beam. Lezgy-Nazargah et al. [14] developed a beam model for the static analysis of composite steel-concrete beams and twin-girder decks which takes into account the effects of shear lag phenomenon as well as the interfacial slip between the concrete slab and steel joists. Lezgy-Nazargah et al. [14] developed a beam model for the analysis of steel mixed-composite beams, taking into account the effects of shear lag and interface slip. Yu et al. [15] developed a model of Twin-cell Composite Box Beam (TCCBB), which is composed of concrete plate and thin-walled steel box beam with twin-cell, is proposed in this paper. Based on established governing differential equations and its relative boundary conditions, closed form solutions of normal stress and shear stress are derived for this TCCBB model; Hu et al. [16] proposed a new type of steel-concrete composite beam with double-box cross-section. In order to investigate stress behaviors and deflection characteristics of such composite beam with wide flange considering the shear lag effect, theoretical analysis and experimental study are launched simultaneously; Miao and Chen [17] proposed an analytical method using full flange width by introducing shear warping shape function and intensity function of the shear warping displacement. The result errors of beam finite element model considering shear-lag effect can be modified by the method. Although scholars have carried out some research on the shear lag effect of composite beams, the theoretical construction is difficult to solve using an analytic method, and the obtained analytical formula is complex, which is not desirable for practical design. In contrast, the widely used finite element numerical method can quickly and accurately analyze the structure, but it is difficult to directly obtain the local internal forces, and it is difficult to analyze the effects of shear lag, warpage, and distortion in the composite beam structure using this method. To this end, an analytical method that can fully reflect the spatial force effects on a composite beam bridge structure that is easy to implement is needed.

Based on the problems discussed above, this paper proposes a new type of spatial grid unit that can be used to analyze the spatial force effect of the composite beam structure, as shown in Fig. 1. Compared with the traditional beam element, the new element has 5 points, more refined analysis characteristics, and obtains internal forces and deformation at multiple locations. At the same time, compared with the traditional plate element, the new element has the characteristics of easier to use, the traditional plate element is difficult to directly obtain the internal force and displacement, but the new element can directly obtain the internal force and displacement of multiple points. By constructing the unit displacement function expression and solving the shape function in combination with the boundary conditions, the total potential energy expression of the space grid element is derived from the minimum potential energy principle [18], and the first order variation is obtained. Finally, the stiffness matrix of the spatial grid unit is obtained. In combination with a MATLAB program [19], the spatial beam unit analysis model of the composite beam is constructed by using the derived spatial grid unit. Because the focus of this paper is the verification

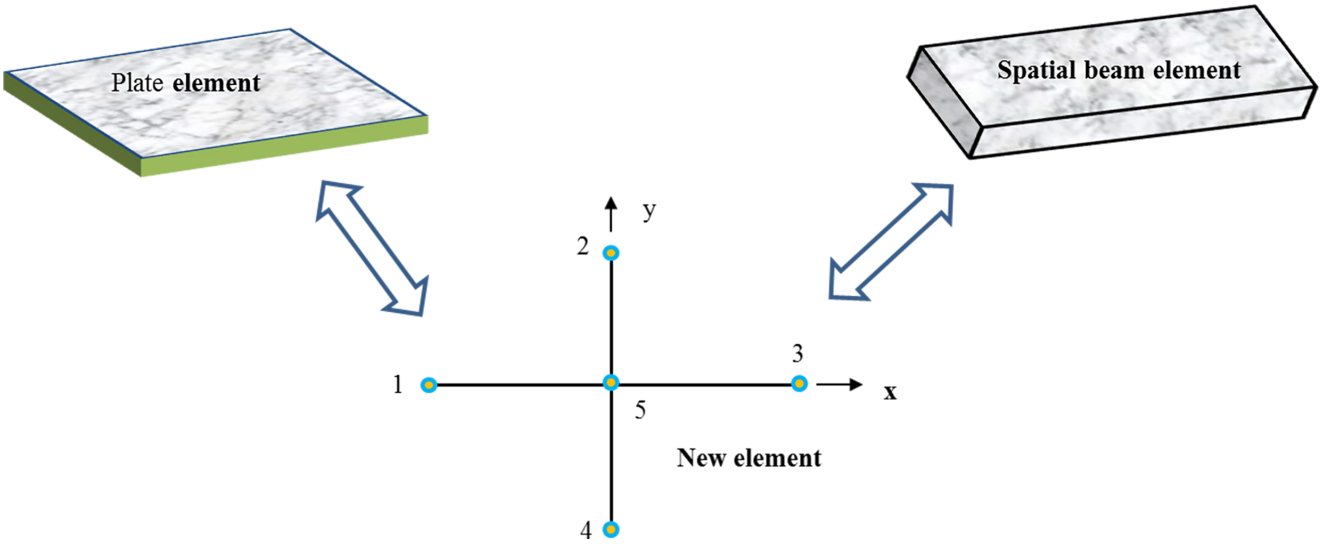

Fig. 1 New element and their comparison

and application of the spatial grid unit model, the slip of the interface will be specifically discussed in subsequent research. Taking the steel-concrete duplex type composite beam as the analysis object, the spatial grid element analysis method is used to study the effects of wide-span ratio, high-span ratio, and web thickness on the shear lag effect of the I-shaped composite beam. Through the sensitivity analysis of different design parameters, the degree of influence and sensitivity of various factors can be determined, which provides a reference for the mechanical behavior analysis and optimization design of composite beams.

2 Derivation of the stiffness matrix of spatial grid elements

2.1 Unit equivalent

As shown in Fig. 1, the spatial grid unit is a 5-node unit with 30 degrees of freedom. When the direct method is used for calculation, it requires a large amount of calculations, and determining the unit stiffness matrix of the spatial grid unit is difficult. Therefore, to facilitate the analysis, the displacement function assumptions of the 51, 52, 53, and 54 beams in the global coordinate system are respectively carried out by using an additional discrete method. According to a given boundary condition, the undetermined coefficient in the displacement function is obtained, and according to the simplified unit displacement function, $V = N\delta^e$, the expression of the shape function N is obtained. Finally, by listing the energy equation $\Pi = U + U_p$ of the overall spatial grid unit, the space element stiffness matrix can be obtained by applying a variation of the minimum potential energy principle.

2.2 Establishment of unit displacement function and solution of shape function

It is assumed that the unit length of the 51 and 53 beams is l_x, the cross-sectional area is A_x, the length of the 52 and 54 beams is l_y, the cross-sectional area is A_y, and the node numbers of the two ends are i and j, respectively, as shown in Fig. 2. The unit coordinate system adopts the right-handed spiral rule, and the X-axis coincides with the central axis of the beam unit. Therefore, the Y-axis and the Z-axis represent the main inertia axes of the beam cross-section. The xy plane and the xz plane are aligned with the cross section such that the bending and shearing in the two planes are independent of each other. The nodal force and nodal displacement of the element are defined by the right-hand spiral rule. In Fig. 2, v_i represents the generalized displacement at the $i(i = 1, 2, \ldots, 12)$ degree of freedom, and f_i represents the generalized force corresponding to the displacement v_i at the i degree of freedom.

The spatial grid unit has five nodes, six degrees of freedom per node, and a total of 30 degrees of freedom.

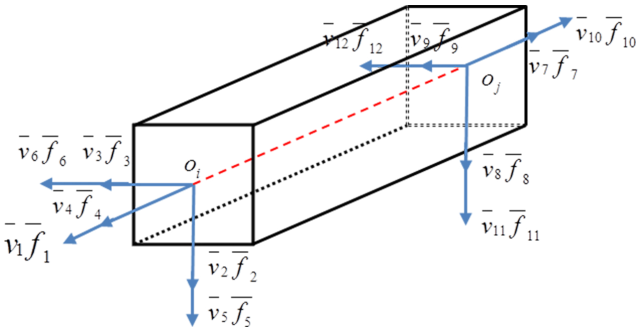

Fig. 2 Nodal forces and nodal displacements of space beam element

The node displacement of the grid unit (30 items in total) is expressed as:

$$\delta^e = \left[u_5, v_5, w_5, \theta_{x5}, \theta_{y5}, \theta_{z5}, \cdots, u_4, v_4, w_4, \theta_{x4}, \theta_{y4}, \theta_{z4}\right]^T. \quad (1)$$

The unit node force (30 items in total) is expressed as:

$$F^e = \begin{bmatrix} N_5, Q_{y5}, Q_{z5}, M_{x5}, M_{y5}, M_{z5}, \cdots, \\ N_4, Q_{y4}, Q_{z4}, M_{x4}, M_{y4}, M_{z4} \end{bmatrix}^T. \quad (2)$$

In Eq. (2), N_i is the axial force; Q_{yi}, Q_{zi} are the shear forces in the y and x directions; M_{xi}, M_{yi}, M_{zi} are the bending moments around the x-axis, y-axis, and z-axis.

To use the node displacement to represent the stress and strain of the element, it must be assumed that the displacement component at any point within the element is a function of the coordinates. When considering the shear deformation, the space grid element considers that the influence of axial deformation and torsional deformation is very low, so it is assumed that the axial displacement function and the angular displacement function are still linear functions of x; for the lateral deflections v and w, a cubic polynomial expression is used owing to boundary condition constraints.

$$V_{ij} = N_{ij}\delta_{ij}^e \quad (3)$$

In the formula, N_{ij} represents the shape function in different displacement deformations, reflecting the geometric deformation shape of the structure and ensuring the continuity of adjacent units.

2.3 Calculation and derivation of element stiffness matrix

When considering the influence of shear deformation, the mesh elements include: axial strain ε_x, bending strains ε_{yy} and ε_{zz}, and shear strains γ_x, γ_y, and γ_z. Taking the 51 and 53 beams of the X axis as an example, according to material mechanics, the various strains can be expressed as:

$$\begin{aligned} &\varepsilon_x = \frac{du}{dx} \quad \varepsilon_{yy} = \frac{d^2v}{dx^2} \quad \varepsilon_{zz} = \frac{d^2w}{dx^2} \\ &\gamma_x = \frac{d\theta_x}{dx} \quad \gamma_y = \frac{kQ_z}{GA} \quad \gamma_z = \frac{kQ_y}{GA} \\ &\varepsilon = \left[\varepsilon_x, \varepsilon_{yy}, \varepsilon_{zz}, \gamma_x, \gamma_y, \gamma_z\right]^T. \end{aligned} \quad (4)$$

The relationship between the stress and displacement of the element can be obtained according to Hooke's law.

$$\sigma_{ij} = \boldsymbol{D_{ij}}\varepsilon_{ij} = \boldsymbol{D_{ij}}\boldsymbol{B_{ij}}\delta_{ij}^e \quad (5)$$

Here, $\boldsymbol{B_{ij}}$ is the generalized geometric matrix of the element, and $\boldsymbol{D_{ij}}$ is the generalized elastic matrix of the element.

From the energy principle, the total potential energy of the object is the sum of the strain energy U of the object and the external force potential U_P, so the total potential energy expression of the element is:

$$\begin{aligned} &\Pi = U + U_P \\ &U = U_{51} + U_{52} + U_{53} + U_{54} \\ &= \frac{1}{2}\begin{bmatrix} \{\delta_{51}\}^{eT}\int_0^{l_x} B_{51}^T D_{51} B_{51} d_x + \{\delta_{52}\}^{eT}\int_0^{l_y} B_{52}^T D_{52} B_{52} d_y \\ + \{\delta_{53}\}^{eT}\int_{-l_x}^{0} B_{51}^T D_{51} B_{51} dx + \{\delta_{54}\}^{eT}\int_{-l_y}^{0} B_{54}^T D_{54} B_{54} dx \end{bmatrix} \\ &U_p = -\{\delta\}^{eT}\{F\}^e. \end{aligned} \quad (6)$$

Here, U is the strain energy of the unit, U_{51}, U_{52}, U_{53}, U_{54} represent the strain energy of each beam, and U_P is the potential energy of the external force.

After obtaining the total potential energy expression, the first potential variation of the total potential energy of the unit is performed by using the principle of minimum potential energy, as follows:

$$\frac{\partial \Pi}{\partial \{\delta\}^e} = 0 \quad (7)$$

resulting in

$$[k]^e\{\delta\}^e = \{F\}^e \quad (8)$$

$$\begin{aligned} [k]^e &= \int_0^{l_x} B_{51}^T D_{51} B_{51} d_x + \int_0^{l_y} B_{52}^T D_{52} B_{52} d_y \\ &+ \int_{-l_x}^{0} B_{53}^T D_{53} B_{53} d_x + \int_{-l_y}^{0} B_{54}^T D_{54} B_{54} d_y. \end{aligned} \quad (9)$$

After calculation, the expressions of $\boldsymbol{B_{ij}}$ and $\boldsymbol{D_{ij}}$ can be obtained as follows:

$$\begin{aligned} &\boldsymbol{B_{ij}} = \left(B_{51}, B_{52}, B_{53}, B_{54}\right);\ \boldsymbol{D_{ij}} = \left(D_{51}, D_{52}, D_{53}, D_{54}\right) \\ &B_{51} = \left[N'_{u51}, N''_{v51}, N''_{w51}, N'_{\theta x51}, N'''_{w51}, N'''_{v51}\right]^T \\ &B_{52} = \left[N''_{u52}, N'_{v52}, N''_{w52}, N'''_{w52}, N'_{\theta y52}, N'''_{v52}\right]^T \\ &B_{53} = \left[N'_{u53}, N''_{v53}, N''_{w53}, N'_{\theta x53}, N'''_{w53}, N'''_{v53}\right]^T \\ &B_{54} = \left[N''_{u54}, N'_{v54}, N''_{w54}, N'''_{w54}, N'_{\theta y54}, N'''_{v54}\right]^T \\ &D_{51} = D_{53} = diag\left(EA_x, EI_z, EI_y, GJ, \frac{b_{zx}l_x^2}{12}EI_y, \frac{b_y l_x^2}{12}EI_z\right) \\ &D_{52} = D_{54} = diag\left(EI_z, EA_y, EI_x, \frac{b_{zy}l_y^2}{12}EI_x, GJ, \frac{b_x l_y^2}{12}EI_z\right). \end{aligned} \quad (10)$$

Substituting $\boldsymbol{B_{ij}}$ and $\boldsymbol{D_{ij}}$ into Eq. (9) and preforming an integral operation, the expression of the space grid

element stiffness matrix considering the shear effect is obtained, and the spatial grid element stiffness matrix can then be obtained.

3 Spatial grid unit model — MATLAB program design and verification

The spatial grid unit is a new spatial analysis unit proposed in this paper. After completing the grid element stiffness matrix derivation, MATLAB is used to develop the analysis program. This allows analysts to save significant time and effort regarding matrix operations, graphics processing, finite element analysis, and additional operations. The model is beneficial for solving the more complicated spatial structure analyses and calculation problems encountered in the research process. The design process of the calculation analysis is shown in Fig. 3.

To verify the correctness and applicability of the spatial mesh element method proposed in this paper, the simple supported box girder analyzed as an example in [20] is selected as the analysis object. The force analysis is carried out by using the space grid element method proposed in this paper. The longitudinal normal stress values of the top and bottom plate joints at the $L/4$ and $L/2$ cross sections are compared with the analytical solutions of the stress values at the corresponding positions given in the literature. The span of the simple supported box girder is 30 m, the dimensions of each part of the box girder are shown in Fig. 4, and the loading condition is a 1 MN/mm^2 uniform load (referred to as the junction load between the top plate and the web of the box girder). The results of the stress analysis are shown in Fig. 5 the longitudinal stress of the top plate and bottom plate of the 30-meter-span box girder structure in the literature is analyzed by using the method proposed in this paper. The analysis results are compared with the test and simulation results in the literature, and the correctness of this paper is verified. At the same time, through the comparison of the simulation analysis results using the traditional simulation analysis element, it is further understood that the new element in this paper is more convenient to directly obtain the internal force and deformation than the traditional plate element, and is more refined than the traditional beam element. The results were compared with those in the literature, under the uniform load of the simple supported box girder,

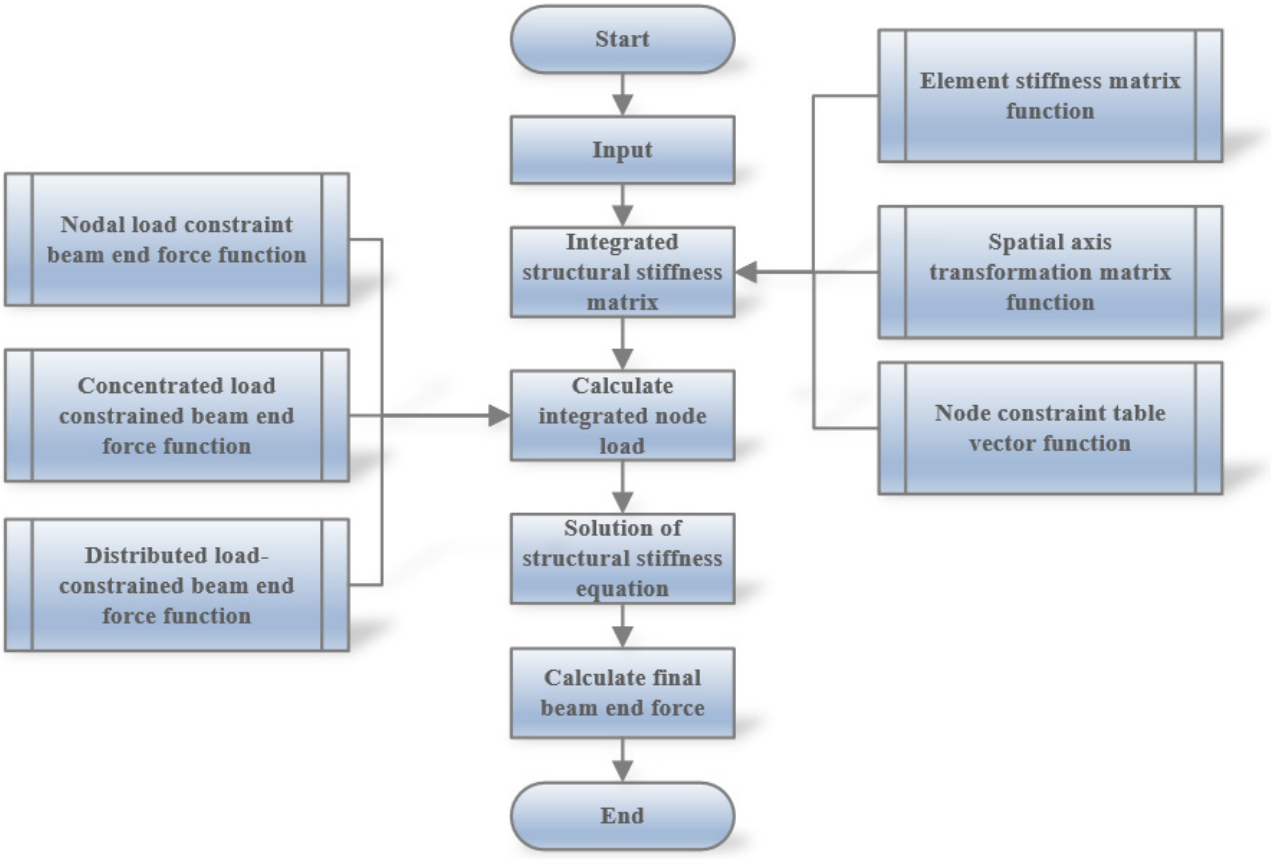

Fig. 3 Analysis and solution process of spatial composite structure grid element model

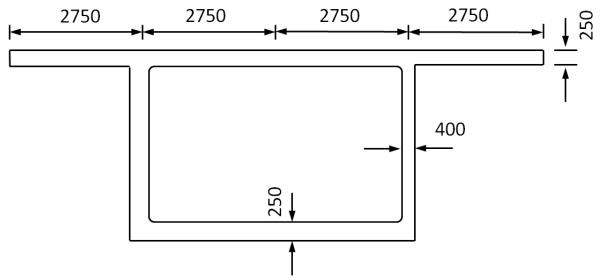

Fig. 4 Box beam cross section (Units: mm)

the maximum stress error of the top plate and the bottom plate at the *L*/2 section is 6.53% compared with the analytical solution presented in the literature. The maximum error at the *L*/4 section is 6.01%, and the positive stress error at most locations is less than 5%.

4 Spatial grid element method application analysis

To verify that the spatial grid element can correctly reveal the spatial force characteristics of the I-shaped composite beam structure, and especially the deformation and stress distribution of the composite beam section, the typical duplex type composite beam is used as the analysis object, and the analysis of the I-shaped composite beam is carried out by applying the spatial grid unit and the MATLAB program. The cross-sectional dimensions (top plate width, web height, web thickness, structural span, etc.) were changed to study the effects of the wide-span ratio, high-span ratio, and web thickness on the shear lag effect of I-shaped composite beams. By analyzing the sensitivity of the parameters, the degree of influence of various factors can be determined. Compared with other analytical

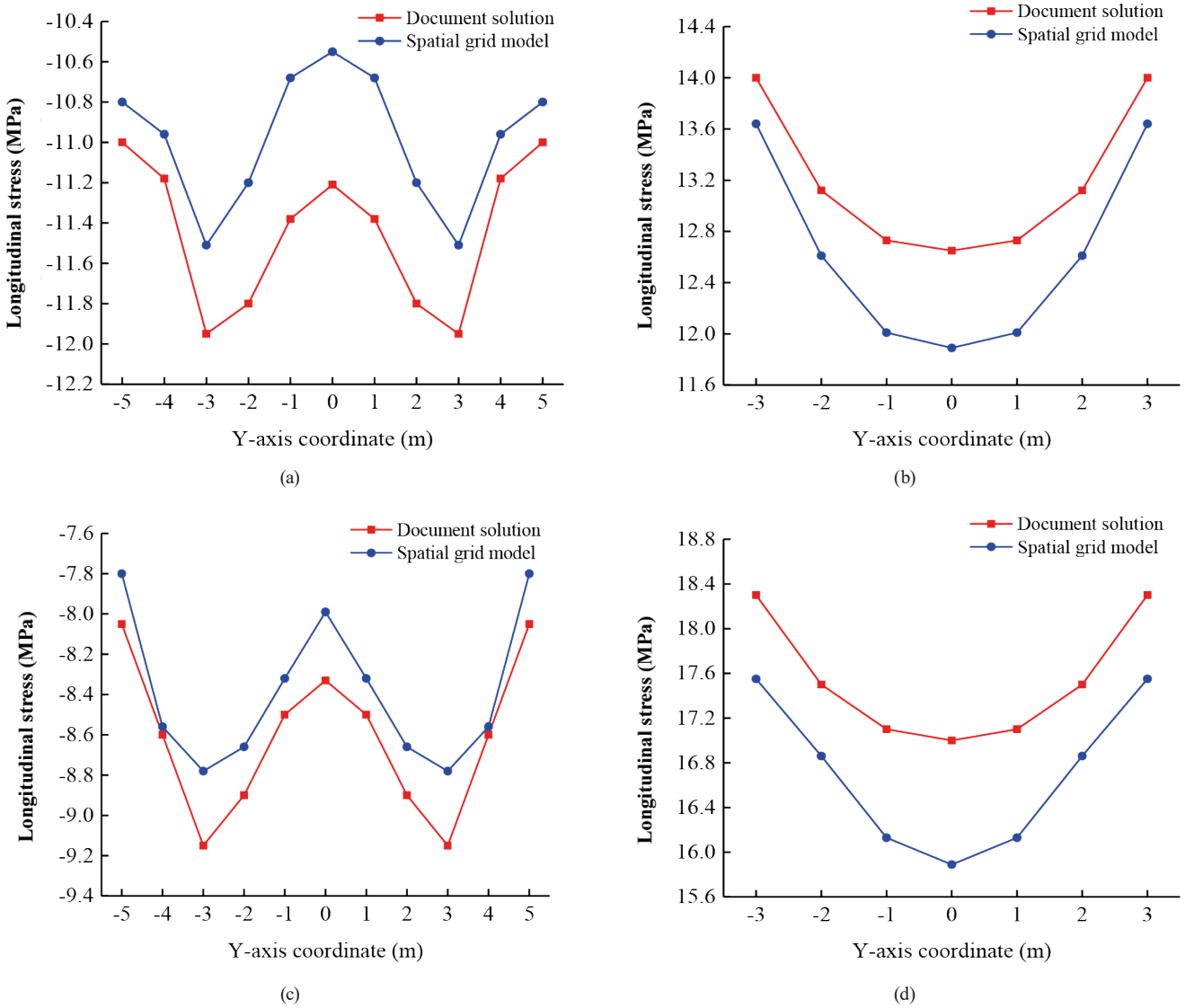

Fig. 5 Results of *L*/2 and *L*/4 section stress analysis: (a) Longitudinal normal stress of the top plate of the *L*/2 section, (b) Longitudinal normal stress of the *L*/2 section bottom plate, (c) Longitudinal normal stress of the top plate of the *L*/4 section, (d) Longitudinal normal stress of the *L*/4 section bottom plate

methods and element types, the spatial grid element analysis method not only obtains the overall and local stress, but also directly outputs various internal forces. Thus, the design provides both structural and local analysis results for application. The cross-sectional dimensions of a typical duplex type composite beam model are shown in Fig. 6. In Fig. 6, $b1$ is the width of the concrete top plate, and $b2$ is the thickness of the lower I-shaped steel web, $h1$ is the thickness of the concrete roof, and $h2$ is the height of the lower I-beam.

4.1 Spatial grid element model for analysis of shearing hysteresis parameters of duplex composite beams

When a steel-concrete I-shaped composite beam is subjected to vertical loads, shear lag occurs [21]. The concept of the shear lag effect coefficient is clearer and more applicable than the concept of the effective distribution width. The coefficient can be applied to the top and bottom plates of concrete box beam sections and various regular steel-concrete composite structures. This study analyzes the shear lag effect using a spatial grid model applied to steel-concrete I-shaped composite beams, and analyzes the influence of different section parameters on the shear lag effect. To facilitate the discussion of the effects on the shear lag effect, this paper introduces the shear lag coefficient, defined as follows:

$$\lambda = \frac{\text{Normal stress considering shear lag effect}}{\text{Normal stress obtained by elementary beam theory}}. \tag{11}$$

4.1.1 Effect of wide-span ratio on shear lag effect

Keeping the width of the composite beam top plate unchanged, and changing the aspect ratio by changing the span of the I-shaped composite beam, the proposed space grid element is used to establish three spatial span I-shaped composite beam models with different spans to reveal the effect of different aspect ratios on the shear lag effect of duplex composite beams. When the spatial mesh model is established, the combined beam section size, boundary conditions, and the number of unit divisions do not change. The size of each unit is changed by changing the size of the dividing unit. The three composite beam models are subjected to a vertical uniform load of 10 kN/m at the joint between the top plate and the web of the I-shaped composite beam. The top plate width of each model is 1000 mm, the top plate thickness is 80 mm, the web height is 400 mm, and the web thickness is 8 mm. The first model has a span of 2000 mm and a width-to–span (or wide-span) ratio of 0.5; the second model has a span of 4000 mm and a wide span ratio of 0.25; and the third model has a span of 6000 mm and a wide-span ratio of 0.17. Table 1 shows the lateral distribution of the stress along the cross section of the steel-concrete I-shaped composite beam for different span ratios.

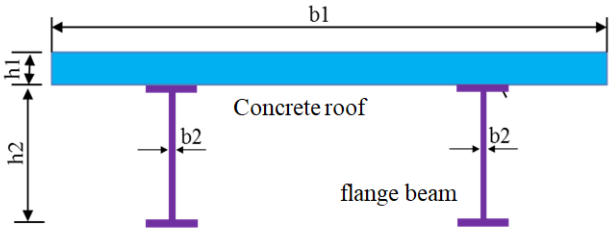

Fig. 6 Dimensions of a steel-concrete double I-beam (mm)

It can be seen from Table 1 that under the uniform symmetric load, the maximum shear lag coefficient of the transverse section of the concrete roof is 1.1143, and the minimum value is 0.7180. When the width-to-span ratio is 0.17, the shear lag coefficient of each point of the transverse section of the concrete roof is 1.028, and the minimum value is 0.9820. As the width-to-span ratio decreases, the shear lag coefficient change interval gradually decreases, and the shear lag effect gradually decreases.

The shear lag coefficient distribution of the steel-concrete duplex type composite beam roof for different width-to-span ratios is shown in Fig. 7, which indicates that the shear lag effect coefficient of each point of the mid-section of the double-shaped composite beam roof plate reaches its maximum at the boundary between the steel web and the roof plate. From the interface between the web and the roof to the edge of the wing and the midpoint of the section, the shear lag coefficient continuously decreases. The shear lag coefficient of the duplex beam reaches its maximum at the intersection of the top plate and the web, and the shear lag coefficient reaches its minimum at the interface. It can be seen that with the gradual reduction of the width-to-span ratio of the steel-concrete duplex type composite beam, the maximum shear lag coefficient of the concrete roof is

Table 1 Shear lag coefficients of roof of steel-concrete double I-beam for different width-span ratios

Width-span ratio	Span of composite beam/mm	Maximum shear lag coefficient	Minimum shear lag coefficient
0.50	2000	1.1143	0.7180
0.25	4000	1.0135	0.9529
0.17	6000	1.0028	0.9820

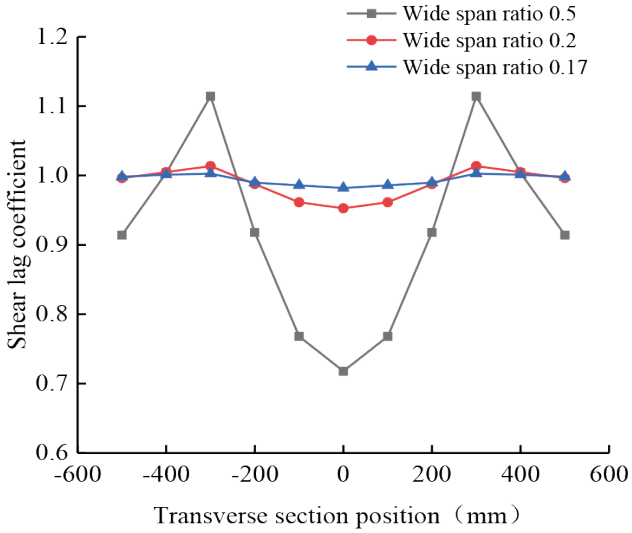

Fig. 7 Shear lag coefficients of roof of steel-concrete double I-beam for different width-span ratios

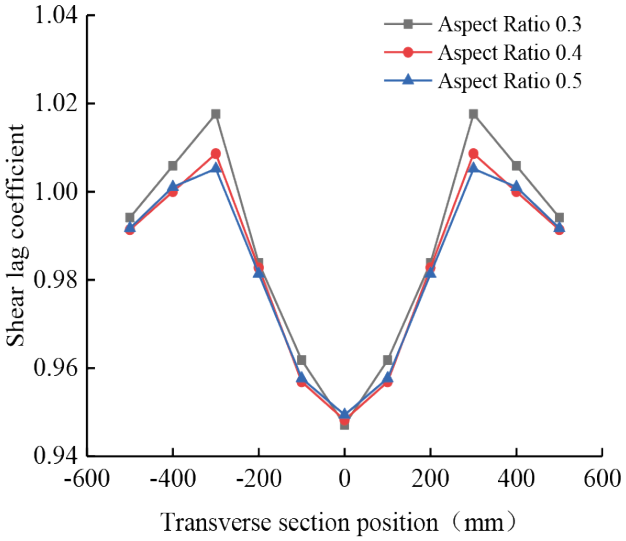

Fig. 8 Shear lag coefficients of roof of steel-concrete double I-beams for different height-width ratios

reduced, and the shear lag effect becomes less obvious. The shear-lag effect for a steel-mixed duplex type beam width span ratio below 0.25 is relatively insignificant.

4.1.2 Effect of aspect ratio on shear lag effect

Keeping the width of the composite beam top plate unchanged, and changing the aspect ratio by changing the height of the I-beam and using space grid elements to establish three spatial span I-shaped composite beam models with different spans, the effect of different aspect ratios on the shear lag effect of duplex composite beams is revealed. The number of unit divisions is constant, the top plate width of each model is 1000 mm, the top plate thickness is 80 mm, the span is 4000 mm, and the web thickness is 8 mm. The first model web is 300 mm high, the aspect ratio is 0.3; the second model web is 400 mm high, the width ratio is 0.4; and the third model web is 500 mm high and the aspect ratio is 0.5. Table 2 shows the lateral distribution coefficients of the stress along the cross section of the steel-mixed I-shaped composite beam for different aspect ratios.

Fig. 8 shows the distribution of the shear lag coefficient for the top plate using different height-width ratio double-shaped composite beams, and Table 2 lists the shear lag coefficients of the roof for different aspect ratios. It can be seen from Fig. 8 and Table 2 that when the aspect ratio is 0.3, the shear lag coefficient changes by 0.0705 between maximum and minimum values, and when the aspect ratio is 0.5, the shear lag coefficient varies by 0.0558. With the gradual increase in aspect ratio, the variation of the shear lag coefficient of the concrete roof gradually decreases.

The variation of the shear lag coefficient of the concrete roof increases with the decrease of the aspect ratio of the steel-concrete duplex type composite beam. The smaller the aspect ratio is, the more significant the shear lag effect. When the aspect ratio of a steel-mixed duplex type composite beam is above 0.4, the shear lag effect is relatively insignificant.

Table 2 Shear lag coefficients of roof of steel-concrete double I-beam for different height-width ratios

Height-width ratio	Web height/ mm	Maximum shear lag coefficient	Minimum shear lag coefficient
0.30	300	1.0176	0.9471
0.40	400	1.0086	0.9482
0.50	500	1.0052	0.9494

4.1.3 Effect of steel web thickness on shear lag effect

By changing the thickness of the composite beam double-shaped steel, the space mesh unit and the space beam unit are used to establish three I-shaped composite beam models with different steel plate thicknesses, and the influence of the web thickness on the shear lag effect of the I-shaped composite beam is revealed. The number of unit divisions is constant, and the top plate width of each model is 1000 mm, the top plate thickness is 80 mm, the span is 4000 mm, and the web height is 400 mm. The first model web thickness is 8 mm, the second model web thickness is 12 mm, and the third model web thickness is 16 mm. Table 3 shows the lateral distribution coefficients of the stress along the cross section for the different web thicknesses.

Fig. 9 shows the distribution of the shear lag coefficient of the double-shaped composite beam for different web thicknesses. Table 3 lists the shear lag coefficients of the

Table 3 Shear lag coefficients of roof of double I-beam for different web thicknesses

Web thickness/mm	Maximum shear lag coefficient	Minimum shear lag coefficient
8	1.0100	0.9496
12	1.0120	0.9473
16	1.0106	0.9526

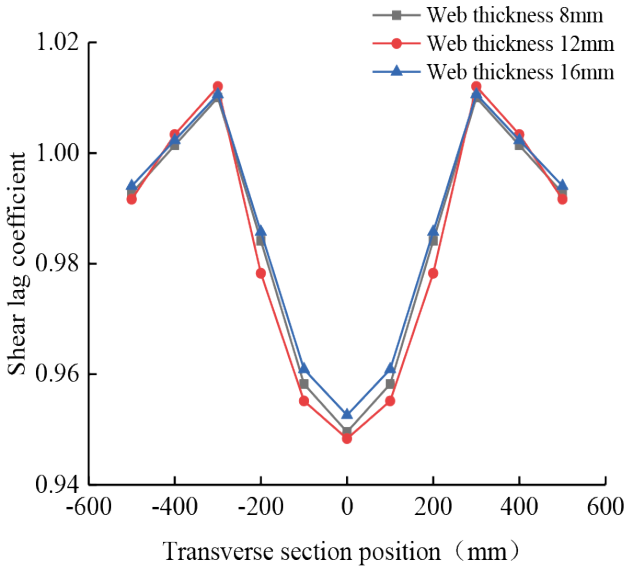

Fig. 9 Shear lag coefficients of roof of different web thicknesses

double-shaped composite beam roof for different web thicknesses. It can be seen from Fig. 9 and Table 3 that when the thickness of the web of the double-shaped composite beam is increased from 8 mm to 16 mm, the maximum value of the shear lag coefficient is approximately 1.01, and the minimum value is approximately 0.95, indicating that the change is small. The results indicate that the shear lag effect of the steel-concrete duplex type composite beam is less affected by any change in the thickness of the steel web.

The parameter analysis of the shear lag effect of the I-shaped composite beam is carried out by applying the grid element to establish the spatial grid model. The analysis results demonstrate that the spatial mesh analysis model using the grid element can accurately reveal the effect of different section parameters on the shear lag effect of the duplex type composite beam. The model can be used for spatial effect analysis and design parameter optimization of steel-concrete composite beams under stress.

4.2 Calculation of internal force and displacement

When designing a composite bridge, it is necessary to analyze both the behavior of each part of the structure under stress and the internal force and deflection of the structure. In the common finite element analysis method, for example, the ANSYS plate and shell element analysis can only extract the stress of different parts, and cannot directly extract the internal force. In the finite section analysis method, only the internal force of the entire section can be extracted, and the internal forces of various parts of the structure cannot be completely reflected. In this study, the internal force analysis of the steel-mixed composite beam is carried out by using the pushed grid unit and the MATLAB program, and the internal forces and displacements of the composite beam roof, floor, and web can be directly obtained in the form of nodal forces and joint deformation. It is also possible to directly obtain the results of the additional deflection of the shear lag effect and the additional internal force.

The steel-concrete duplex type composite beam is used as an example, and the load is 20 kN/m, symmetrically distributed across the span. The specific section size and the load form are shown in Fig. 10. Tables 4 and 5 respectively show the deflection and bending moment of each joint along the span direction of the top plate and the web under the symmetric distributed load. The details are as follows.

Through the numerical analysis of the composite beam space grid element method, it is found that the spatial grid element method can extract the stress of the nodes in all directions, and can extract the displacement and internal force values of the nodes in different directions. It can be seen from the results for internal force and deformation that because the calculation result is output by the unit node force. It is also possible to extract the rotation angle, bending moment, and torque of each node at different

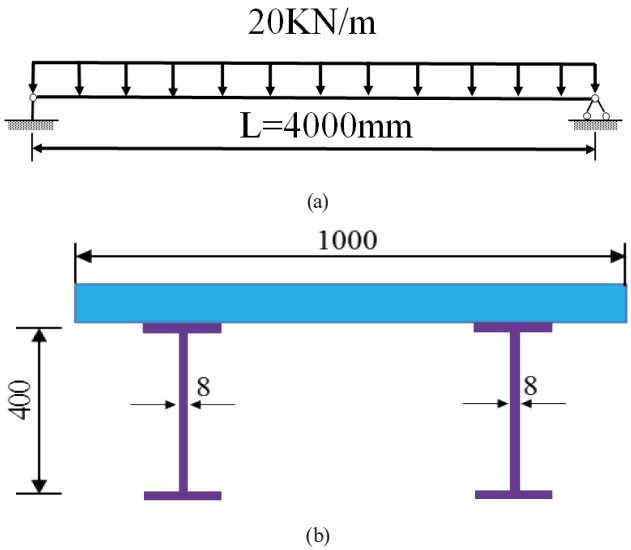

Fig. 10 Combined double I-beam subjected to symmetrical distributed load: (a) Load elevation, (b) Duplex type composite beam section size/mm

Table 4 Partial deflection of the intersection of the composite beam roof and the steel web (units: mm)

Coordinates in X direction/ mm	Deflection of elementary beam theory δ_0	Deflection of space grid element δ_1	Shear lag additional deflection $\delta_2 = \delta_1 - \delta_0$	δ_2/δ_0/%
200	-1.596E-04	-1.656E-04	-5.955E-06	3.73%
400	-2.836E-04	-2.965E-04	-1.290E-05	4.55%
600	-4.099E-04	-4.206E-04	-1.070E-05	2.61%
800	-5.105E-04	-5.343E-04	-2.379E-05	4.66%
1000	-6.146E-04	-6.348E-04	-2.016E-05	3.28%
1200	-6.951E-04	-7.199E-04	-2.481E-05	3.57%
1400	-7.568E-04	-7.879E-04	-3.110E-05	4.11%
1600	-7.997E-04	-8.374E-04	-3.774E-05	4.72%
1800	-8.307E-04	-8.675E-04	-3.680E-05	4.43%
2000	-8.419E-04	-8.775E-04	-3.561E-05	4.23%

Table 5 Partial bending moment of the intersection of the composite beam (units: KN * m)

Coordinates in X direction/ mm	Bending moment: elementary beam theory M_0	Bending moment: space grid element M_1	Shear lag additional bending moment $M_2 = M_1 - M_0$	M_2/M_0/%
200	7.6	7.902	0.302	3.97%
400	14.4	15.101	0.701	4.87%
600	20.4	21.345	0.945	4.63%
800	25.6	26.793	1.193	4.66%
1000	30	31.584	1.584	5.28%
1200	33.6	35.136	1.536	4.57%
1400	36.4	38.624	2.224	6.11%
1600	38.4	41.364	2.964	7.72%
1800	39.6	42.938	3.338	8.43%
2000	40	43.344	3.344	8.36%

positions, and the result of the internal force of the shear force hysteresis effect can be directly obtained, which is difficult to obtain from other finite element numerical analysis methods. The effects of additional deflection and additional bending moment caused by the shear lag effect can be analyzed using the proposed method. The analysis results indicate that the additional deflection of shear lag represents 4.72% of the total deflection of the elementary beam and that the additional bending moment of the shear lag can reach up to 8.43% of the total bending moment of the elementary beam.

5 Conclusions

In this paper, the energy matrix principle is used to derive the stiffness matrix of the proposed space grid element. Combined with the developed MATLAB finite element analysis program, the steel-concrete duplex type composite beam is taken as the analysis object. By changing the section parameters, the effects of different wide-span ratios, high-span ratios, and web thicknesses on the shear lag effect of duplex type composite beams are analyzed. At the same time, based on the analysis of shear lag parameters, the analysis of additional internal force and deformation caused by the shear lag effect is carried out. The main conclusions are as follows:

1. The shear lag effect on a steel-concrete duplex type composite beam increases with increasing wide-span ratio and it increases with decreasing aspect ratio, while the effect of shear lag effect changes little with variations in web thickness. This conclusion is consistent with existing research conclusions, indicating that the spatial grid element analysis method can effectively analyze the spatial effects of steel-mixed composite beams under stress.
2. Using the analysis method to calculate the internal force and displacement of different parts of the steel-concrete duplex type composite beam under the action of a symmetric distributed load indicates that the spatial grid element analysis method can directly obtain the local stress, internal force, and

displacement of various parts. It is also possible to extract the rotational angles, bending moments, and torques of the various nodes at different positions, and to directly obtain the internal forces such as shear lag, warpage, and distortion effects.

3. The analysis results of the duplex type composite beam presented in this paper indicate that the additional deflection of the shear force lag contributes up to 4.72% to the total deflection of the elementary beam and that the additional bending moment of the shear force lag contributes up to 8.43% to the total bending moment of the elementary beam. Because the shear lag effect can significantly affect the actual stress distribution of a composite structure if it is not comprehensively considered, the deflection and stress generated by an external load on the composite beam structure may be underestimated, resulting in safety hazards related to instability and potential local damage of the composite beam structure. Therefore, the shear lag effect should be carefully considered in composite structure designs.
4. The derivation process of the energy variation method is clear, simple, and easy to program. It is not only suitable for analysis using spatial grid cells, but can be used for analysis and calculation using other types of cells and even structures. It has good application value, especially regarding the interface beam slip effect of composite beams. In subsequent research, by adding an interface spring unit to form a new type of space grid unit, the theoretical simulation analysis and engineering application involving the static, dynamic, and stability of some composite beams can be carried out. Because the focus of this paper is the verification and application of the spatial grid element model, the I-beam composite beam interface is coupled by the unit node degree of freedom; therefore, the interface slip will be specifically discussed in a subsequent study.

In summary, the spatial grid element analysis method can accurately, reliably, and quickly evaluate the steel-mixed composite structure. It has important theoretical value and engineering application significance for the effective analysis and application of composite bridge structures.

Acknowledgements

The authors gratefully acknowledge the financial support provided the Science and Technology Project of Zhejiang Provincial Department of Transportation (Grant No. 2018010, 2019H17 and 2019H14) and A Project Supported by Scientific Research Fund of Zhejiang Provincial Education Department (Grant No. Y202250418). The Science and Technology Agency of Zhejiang Province (Grant No. LTGG23E080006). Jiaxing Science and Technology Bureau of China under Grant (2023AY11020).

Author contributions

All authors designed the study, collected data, wrote the manuscript and revised it. Pengzhen Lu put forward a concept, Yu Ding model analysis, Zhenyi Qi data analysis, Ying Wu Method improvement, Liu Yang verification, Yang Li theoretical analysis.

Data availability

Some or all data, models, or code generated or used during the study are available from the corresponding author by request.

Declarations

Conflict of interest: There is no conflict of interest.

Consent to participate: All authors designed the study, collected data, wrote the manuscript and revised it.

Consent to publish: All authors agree to publish this manuscript. There is no conflict of interest.

Ethical approval: The present study and ethical aspect was approved by School of Civil Engineering, Zhejiang University of Technology, Hangzhou 310023, China.

References

[1] Nie, J. G., Tao, M. X., Wu, L. L., Nie, X., Li, F. X., Lei, F. "Advances of research on steel-concrete composite bridges", China Civil Engineering Journal, 45(6), pp. 110–122, 2012.

[2] Huang, D., Wei, J., Liu, X., Zhang, S., Chen, T. "Influence of post-pouring joint on long-term performance of steel-concrete composite beam", Steel and Composite Structures, 28(1), pp. 39–49, 2018.
https://doi.org/10.12989/scs.2018.28.1.039

[3] Tian, S.-P. "Research on the calculation of shear connector of steel concrete composite beam", Journal of Railway Engineering Society, 31(8), pp. 56–61, 2014.

[4] Su, Q., Dai, C., Xu, C. "Full-Scale Experimental Study on the Negative Flexural Behavior of Orthotropic Steel–Concrete Composite Bridge Deck", Journal of Bridge Engineering, 23(12), 04018097, 2018.
https://doi.org/10.1061/(ASCE)BE.1943-5592.0001320

[5] Elmy, M. H., Nakamura, S. "Static and seismic behaviours of innovative hybrid steel reinforced concrete bridge", Journal of Constructional Steel Research, 138, pp. 701–713, 2017. https://doi.org/10.1016/j.jcsr.2017.08.025

[6] Liu, H. C., Wan, S., Liu, Q. J. "Study on the Pure Torsion Performance of I-Type Steel-Concrete Composite Bridge with Double Girders", IOP Conference Series: Materials Science and Engineering, 269, 012054, 2017. https://doi.org/10.1088/1757-899X/269/1/012054

[7] Kisała, D., Furtak, K. "The assessment of the slip influence on the deflection of the steel plate-concrete composite beams", Archives of Civil Engineering, 62(2), pp. 59–76, 2016. https://doi.org/10.1515/ace-2015-0065

[8] Zhang, G., Kodur, V., Yao, W., Huang, Q. "Behavior of composite box bridge girders under localized fire exposure conditions", Structural Engineering and Mechanics, 69(2), pp. 193–204, 2019. https://doi.org/10.12989/sem.2019.69.2.193

[9] Tong, Z., Song, X., Huang, Q. "Deflection calculation method on GFRP-concrete-steel composite beam", Steel and Composite Structures, 26(5), pp. 595–606, 2018. https://doi.org/10.12989/scs.2018.26.5.595

[10] Zou, G. P., Xia, P. X., Shen, X. H., Wang, P."Mechanical properties analysis of steel-concrete-steel composite beam", Journal of Sandwich Structures & Materials, 19(5), pp. 525–543, 2017. https://doi.org/10.1177/1099636215622949

[11] Liu, J., Ding, F., Liu, X., Yu, Z. "Study on flexural capacity of simply supported steel-concrete composite beam", Steel and Composite Structures, 21(4), pp. 829–847, 2016. https://doi.org/10.12989/scs.2016.21.4.829

[12] Zhu, L., Su, R. K. L. "Analytical solutions for composite beams with slip, shear-lag and time-dependent effects", Engineering Structures, 152, pp. 559–578, 2017. https://doi.org/10.1016/j.engstruct.2017.08.071

[13] Luo, D., Zhang, Z., Li, B. "Shear lag effect in steel-concrete composite beam in hogging moment", Steel and Composite Structures, 31(1), pp. 27–41, 2019. https://doi.org/10.12989/scs.2019.31.1.027

[14] Lezgy-Nazargah, M., Vidal, P., Polit, O. "A sinus shear deformation model for static analysis of composite steel-concrete beams and twin-girder decks including shear lag and interfacial slip effects", Thin-Walled Structures, 134, pp. 61–70, 2019. https://doi.org/10.1016/j.tws.2018.10.001

[15] Yu, J., Hu, S. W., Xu, Y. C. Fan, B. "Coupled Mechanism on Interfacial Slip and Shear Lag for Twin-Cell Composite Box Beam Under Even Load", Journal of Mechanics, 34(5), pp. 601–616, 2018. https://doi.org/10.1017/jmech.2017.77

[16] Hu, S.-W., Yu, J., Huang, Y.-Q., Xiao, S.-Y. "Theoretical and Experimental Investigations on Shear Lag Effect of Double-Box Composite Beam with Wide Flange under Symmetrical Loading", Journal of Mechanics, 31(6), pp. 653–663, 2015. https://doi.org/10.1017/jmech.2015.31

[17] Miao, L., Chen, D. W. "The Effect of Shear Lag on Long-Term Behavior of Steel/Concrete Composite Beams", Advanced Materials Research, 255–260, pp. 1070–1076, 2011. https://doi.org/10.4028/www.scientific.net/AMR.255-260.1070

[18] Gan, Y., He, Z., Rong, T., Zhou, G. "Energy-variational method for the analysis of shear lag effect of thin-walled curved I-beams with wide flange", Engineering Mechanics, 27(12), pp. 1–7, 2010.

[19] Zhou, S., Chen, S. "Matlab application to the matrix deduction of finite element stiffness", Journal of Chongqing Jiaotong University(Natural Science), 26(2), pp. 29–31, 2007.

[20] Qin, X., Liu, H. "Effective flange width of simply supported box girder under uniform load", Acta Mechanica Solida Sinica, 23(1), pp. 57–65, 2010. https://doi.org/10.1016/S0894-9166(10)60007-9

[21] Jiang, R. J., Xiao, Y. F., Yi, X. W., Wu, Q. M., Gai, W. M."Study on the shear lag effect of the PC box girder bridge with corrugated steel webs under concentrated loads", Applied Mechanics and Materials, 644–650, pp. 5054–5060, 2014. https://doi.org/10.4028/www.scientific.net/AMM.644-650.5054